Proc. NIPR Symp. Upper Atmos. Phys., **11**, 61–71, 1998

PERIODIC LF WAVE RADIATION ASSOCIATED WITH PULSATING AURORA

Hirokazu TAKIZAWA[1], Akira MORIOKA[1], Hiroaki MISAWA[1] and Hiroshi MIYAOKA[2]

[1]*Upper Atmosphere and Space Research Laboratory, Tohoku University, Sendai 980-8578*
[2]*National Institute of Polar Research, 9–10, Kaga 1-chome, Itabashi-ku, Tokyo 173-8515*

Abstract: The pulsating aurora accompanied with LF waves was found from the observation by the ground-based SIT all-sky TV and a sounding rocket S-520-12 launched from Andøya, Norway at 0206:00 UT on February 26, 1990. On the basis of the correlation analysis, the LF waves lagged behind auroral emission by 8 s. This evidence is explained by the assumption that the pulsating LF waves were generated by precipitating low energy electrons modulated near the magnetic equator simultaneously with high energy auroral electrons causing the auroral emission. It was also derived from the ray tracing method, that the LF waves were generated in the altitude range from 2000 km to 4700 km along the magnetic field line of $L=6.7$ on which pulsating auroral patch existed.

1. Introduction

A pulsating aurora is a kind of most common aurora, which appears predominantly from the midnight through the morning as a weak diffuse aurora (ROYRVIK and DAVIS, 1977), during the recovery phase of substorm (OGUTI, 1981). Pulsating auroras show complex shapes and motions with quasi-periodic intensity fluctuations at each auroral patch. The pulsation period is typically about 10 s (YAMAMOTO and OGUTI, 1982). Although the morphological features of pulsating auroras are well studied, there remain essential questions on the source of precipitating electrons, the mechanism of periodic precipitation, and the process governing the pulsating period.

Pulsating auroras have been observed by various ground-based observations and *in-situ* rocket experiments. BRYANT *et al.* (1971) reported, on the basis of the simultaneous observation by a ground-based photometer and rocket-borne measurements, that periodic luminosity variations are caused by the precipitating electrons in the energy range between several keV and several tens of keV, and that there is a time dispersion between different electron energies. They showed that the time dispersion relation is well interpreted by the source modulation at the magnetic equator. In the later measurement by YAU *et al.* (1981), the time dispersion of precipitating electrons was also observed. Several investigations on electromagnetic waves related to pulsating auroras have been carried out. TSURUTANI and SMITH (1974) observed ELF (10–1500 Hz) chorus pulsations with quasi-period of 5–15 s near magnetic equatorial region from $L=5$ to $L=9$, and they suggested that modulations of the chorus intensity in the

postmidnight region might cause modulations of the energetic electron precipitation. TSURUDA *et al.* (1981) reported that there was a good correlation between the VLF (1–5 kHz) chorus observed with a crossed-loop antenna and pulsating aurora observed simultaneously by a low-light-level TV camera. The direct correspondence between whistler mode waves in the magnetospheric/ionospheric region and the pulsating aurora has not been detected. In this paper, we present the evidence that the pulsating aurora caused by higher energy electron is associated with the LF wave modulation generated by lower energy electrons.

2. Observation

Two Japanese sounding rockets, S-520-12 and S-520-14 were launched at Andøya Rocket Range, Norway (69.32°N, 16.02°E in geodetic; 67.25°N, 114.38°E in geomagnetic), on February 26, 1990 and February 12, 1991, respectively. The data used in this study are obtained by the first launching with the S-520-12 rocket. The purpose of the S-520-12 rocket experiment was to study the electromagnetic and optical processes occurring within a pulsating aurora in cooperation with the ground-based SIT-TV observations. For this purpose, seven kinds of instruments were installed in S-520-12; for plasma wave measurement in the high frequency range (PWH), very low frequency plasma wave experiment (VLF), electron density measurement by an impedance probe (NEI), magnetic field experiment (MGF), DC electric field detector

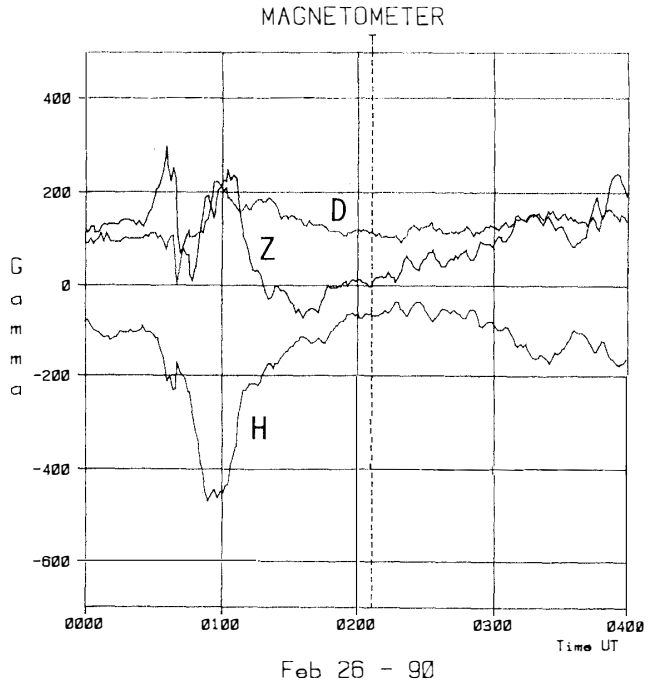

Fig. 1. Geomagnetic condition on February 26, 1990, at Andøya, Norway. The S-520-12 rocket was launched at 0206:00 UT (0506:00 MLT), when the geomagnetic condition was in the recovery phase of a substorm (dashed line).

(EFD), electron measurement (ESP), and ion energy mass spectrometer (IMS). The S-520-12 rocket was launched into a diffuse aurora at 0206:00 UT (0506:00 MLT) on February 26, 1990, when a pulsating aurora was moderately active above the station, and the geomagnetic condition was in the recovery phase of a substorm (Fig. 1). The spin and coning period of the rocket were 1.587 s and 140 s, respectively. The PWH measured electric field spectrum of plasma waves in a wide frequency range from 20 kHz up to 5 MHz in every 1.28 s with a dipole whip antenna ($2m \times 2$). The PWH had two frequency sweep modes, and data sampling time was 2.56 s. Simultaneous auroral image data by ground-based SIT-TV camera was obtained during the time period from 0206:00 UT to 0221:00 UT. The all-sky TV image was recorded as analogue video data. The digitization of the video data was carried out by the ARSAD (Automatic Retrieval System for Auroral Data) installed at Aurora Data Center in NIPR. The TV image data was digitized with a sampling rate of 1 s and a spatial resolution of 320 *pixels*×240 *pixels*.

3. Pulsating Aurora and LF Waves

The dynamic (frequency-time) spectrum of LF plasma waves measured by the PWH onboard the S-520-12 rocket is shown in Fig. 2. In the frequency range from 60 kHz to 140 kHz quasi-periodic broadband emissions can be seen in the figure. In this frequency range, the wave intensity at 139 kHz band was taken as a representative of the LF wave activity in the following analysis. The 139 kHz LF wave inten-

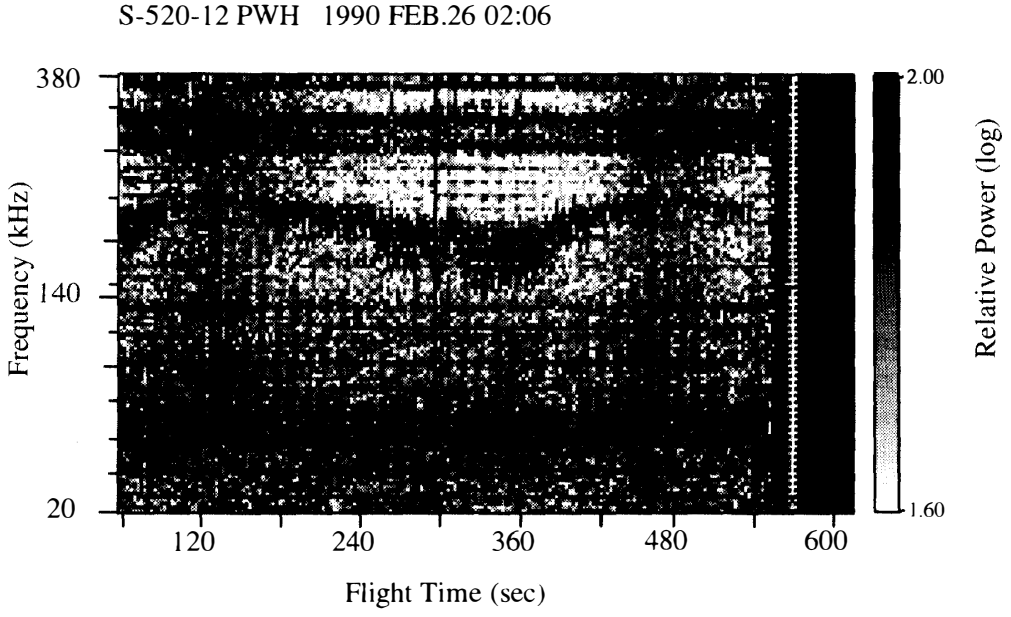

Fig. 2. The dynamic (frequency-time) spectrum of LF (20 kHz–380 kHz) plasma waves measured by the PWH onboard the S-520-12 rocket. Quasi-periodic broadband emissions can be seen in the frequency range from 60 kHz to 140 kHz, in the time range from t=60 s to t=540 s.

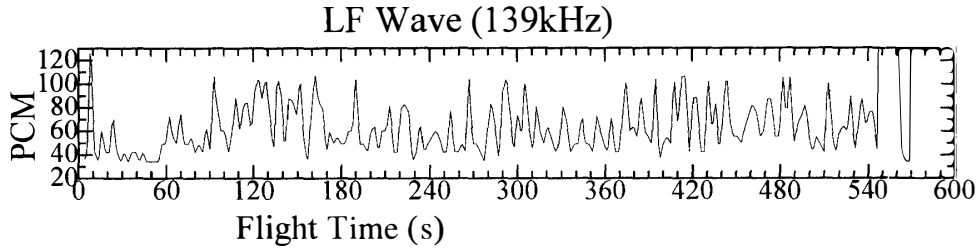

Fig. 3. The intensity variation of LF waves at 139 kHz band. Quasi-periodic emissions can be seen with the period of approximately 10 s.

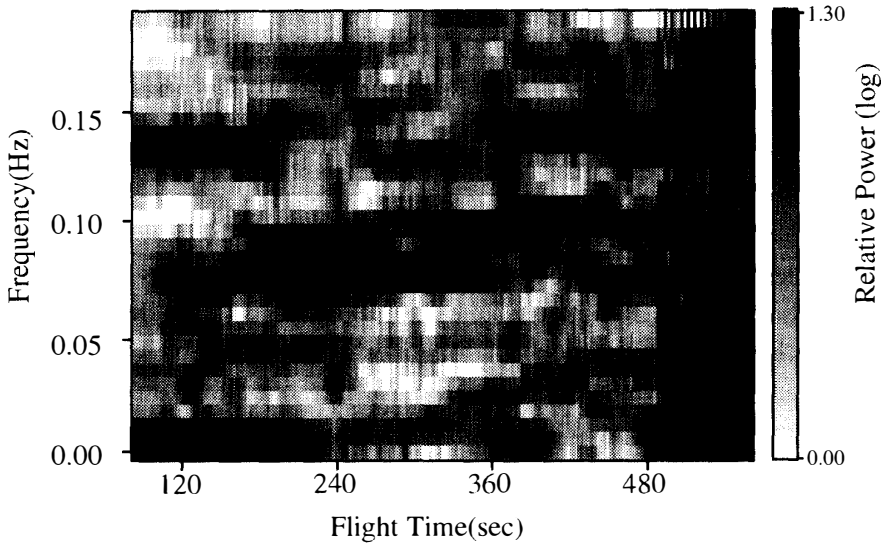

Fig. 4. The dynamic (frequency-time) spectrum of the 139 kHz LF wave intensity variation. The intensity varied periodically with dominant period from 10.0 s (0.10 Hz) to 14.3 s (0.07 Hz).

sity varied periodically during the rocket flight (Fig. 3). The dynamic spectrum of the 139 kHz LF wave variation is shown in Fig. 4. The intensity of LF wave at 139 kHz showed periodical variation with dominant period from 10.0 s (0.10 Hz) to 14.3 s (0.07 Hz) from 0208:00 UT (t=120 s after the launch) to 0214:00 UT (t=480 s). It must be kept in mind for the later discussion that the typical period of LF wave around t=240 s is about 11.7 s (0.085 Hz). As for plasma waves in very low frequency range measured by VLF instrument onboard the S-520-12 rocket, we cannot find out periodic intensity variations with about 12 s, because the VLF instrument changed its gain every 10 s.

During the rocket flight, many pulsating auroral patches appeared and disappeared in the field of view above the station. Therefore, it is generally impossible to study which auroral patch or patches would be responsible for LF pulsations observed by the rocket. However at around 240 s of the flight time (0210:00 UT), only one pulsating auroral patch existed near the zenith for about 12 s. Thus, the time period around t=240 s is the sole chance to study the relationship between the propagating LF wave

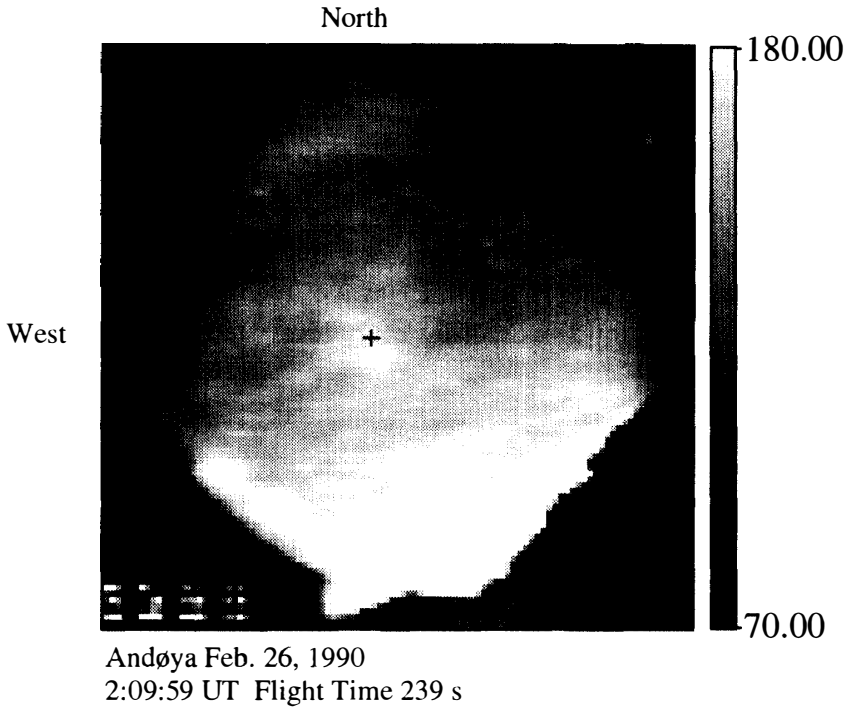

Fig. 5. The all-sky TV image at $t=239$ s observed ground-based SIT-TV camera. The location of the pulsating auroral patch in question is indicated by a cross near the zenith. The crosses in the north-west quadrant in the field of view indicate the rocket locations at $t=220$ s, 240 s, and 260 s projected down to the 100 km altitude along the geomagnetic field line.

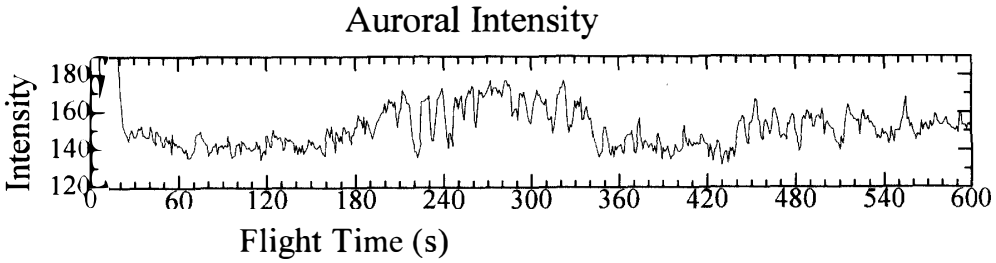

Fig. 6. The auroral luminosity at a point near the zenith, with its quasi-periodic variation from $t=220$ s to $t=260$ s during the rocket flight.

obtained by the rocket and pulsating aurora recorded simultaneously by the ground-based SIT-TV camera. Figure 5 shows the all-sky TV image at $t=239$ s. The location of the pulsating aurora is indicated by a cross near the zenith. The locations of the rocket at $t=220$ s, 240 s, and 260 s projected down to the 100 km altitude along the magnetic field line are also indicated by crosses in the north-west region. The location of the rocket at $t=240$ s was about 160 km away from the pulsating auroral patch near the zenith. Figure 6 shows the auroral luminosity at the zenith during the rocket flight, which demonstrates a periodical luminosity variation around $t=240$ s. The dynamic spectrum of auroral intensity variation near the zenith in Fig. 7 shows us a clear period of 11.6 s (0.086 Hz) in the auroral intensity around $t=240$ s, which just

coincides with the period of the LF wave modulation (11.7 s). This evidence strongly suggests that the isolated auroral patch near the zenith was closely related with the generation of the pulsating LF waves.

To investigate the phase relation between the pulsating aurora and LF wave modulation, the cross-correlation analysis was performed. Figure 8 shows the dynamic cross-correlation diagram during the rocket flight. As a result of this correlation analysis, it becomes apparent that the pulsating aurora and LF waves have a steady phase relation around $t=240$ s, and the 139 kHz LF wave intensity lags behind 8 s or leads 4 s to the pulsating auroral intensity during the period analyzed.

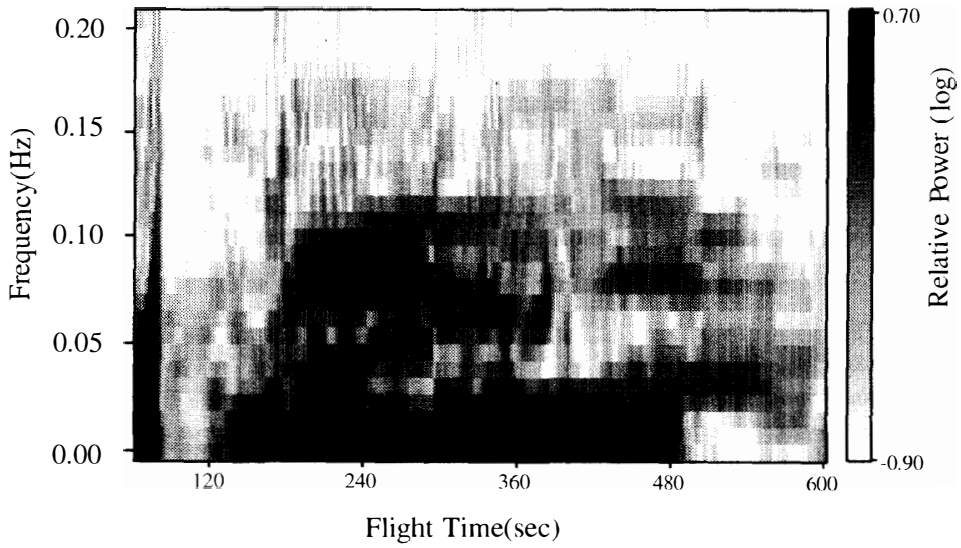

Fig. 7. The dynamic (frequency-time) spectrum of auroral luminosity variation near the zenith around t=240 s showing a clear period of 11.6 s (0.086 Hz).

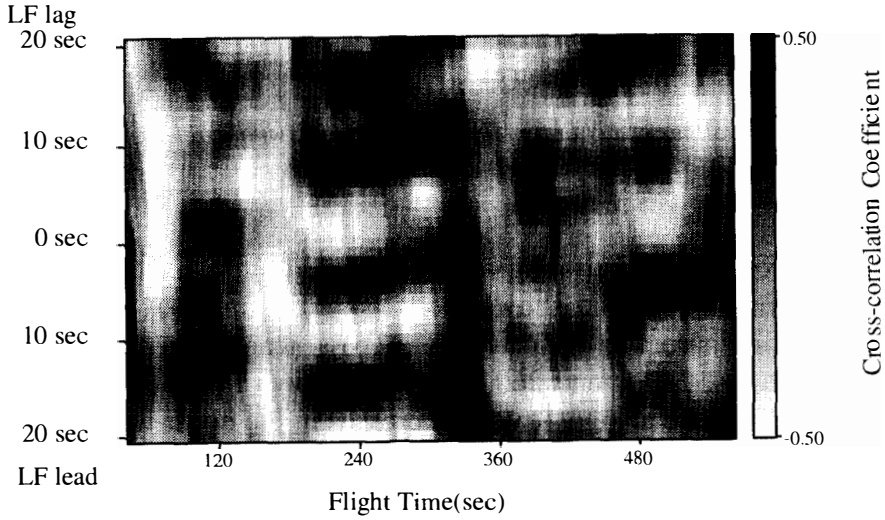

Fig. 8. The dynamic cross-correlation diagram between the pulsating aurora and LF wave modulation during rocket flight time. The LF wave shows an obvious lag time of 8 s or leading time of 4 s to pulsating auroral intensity around t=240 s.

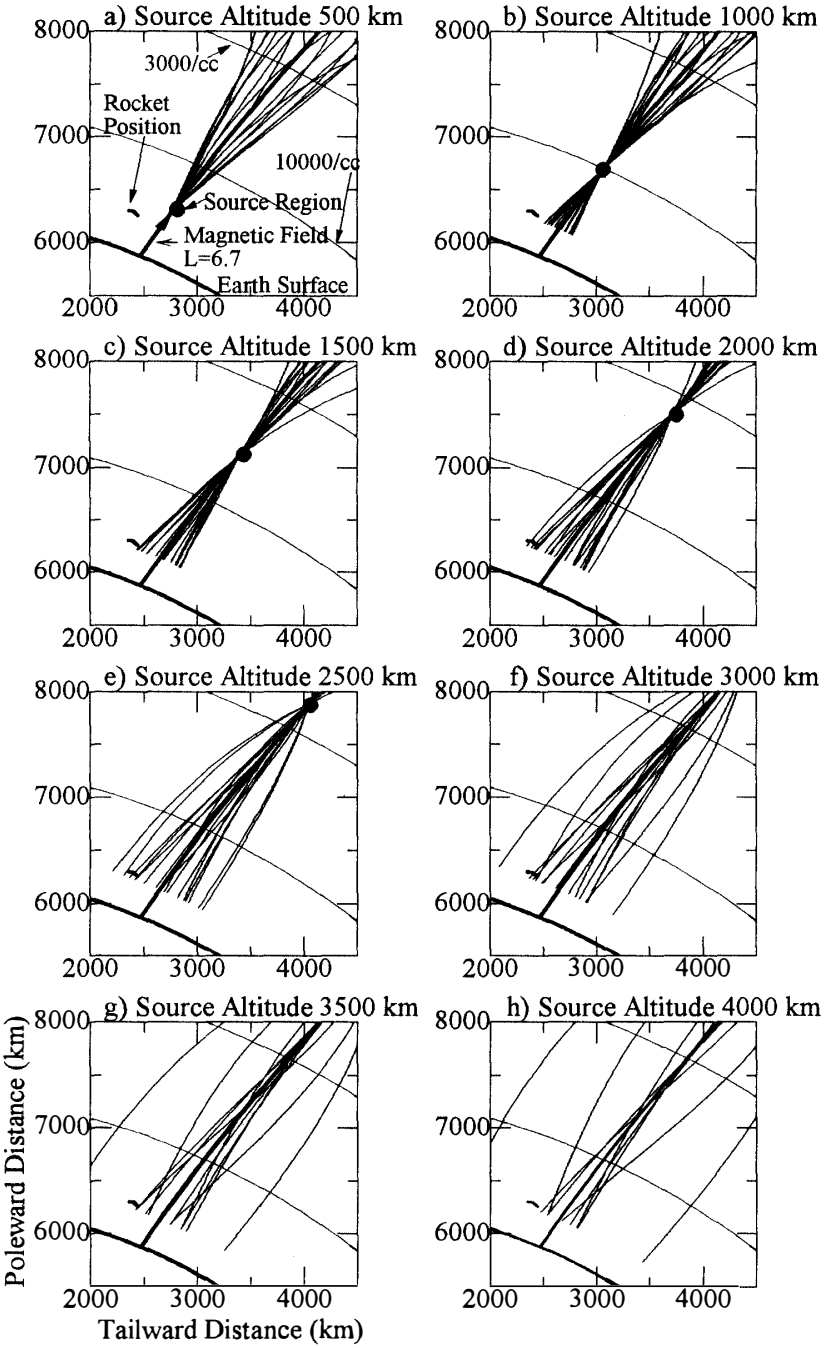

Fig. 9. The ray paths of LF waves at 139 kHz generated on the field line of L=6.7. The source altitude is taken with 500 km steps from 500 km (a) to 4000 km (h). The figure also shows the rocket position during the period from t=220 s to t=260 s, earth surface, magnetic field line of L=6.7, and electron density contours expressed by eq. (1).

The region of the LF wave generation is investigated using a ray tracing method. Auroral electrons precipitate along magnetic field lines, and LF waves generated by these precipitating electrons can propagate straying from the field lines. On the assumption that LF waves are generated on an $L=6.7$ magnetic field line with pulsating electrons and resultant aurora, we made a ray tracing analysis of LF waves, to estimate the generating altitude. Our calculation for ray paths of the whistler mode waves adopted an electron density model based on the observation by the ISIS 1 satellite (BENSON *et al.*, 1980), *i.e.*,

$$N=10^4\times\exp\left(1-\frac{H}{1000}\right)\quad(\mathrm{cm}^{-3}). \tag{1}$$

where H (km) is altitude. An earth-centered dipole model is used for the magnetic field, and the space medium is treated as cold and collisionless plasma. Parameters in our calculation are the wave generating altitude, wave normal angle with respect to the magnetic field. The results of ray tracings with changing their start points (source altitude) by 500 km are shown in Fig. 9, where wave normal angle with respect to the magnetic field is basically scanned by 10° step between 0° and 360°, and traces of ray paths at 139 kHz are shown. In addition to these basic 10° step ray paths, the downward ray paths located at the highest or the lowest latitude are also plotted in the figure to show the region in which LF waves can be observed. The rocket position during the period from $t=220$ s to $t=260$ s, earth surface, magnetic field at $L=6.7$, and electron density contours expressed by eq. (1) are also shown in the figure. When the source altitude is 500 km, the ray of 139 kHz wave cannot reach the rocket position, so that the rocket could not measure LF waves generated on the magnetic field of $L=6.7$ with the pulsating aurora. The cases of the source altitude of 1000 km and 1500 km are similar to the case of 500 km. When the source altitude is 2000 km, the ray path crosses the rocket position, so that the rocket would measure LF waves. The cases of source altitudes higher than 2500 km (e~h) also show that rays can reach the rocket. However, when the source altitude is higher than 4700 km, the LF wave frequency exceeds the local electron plasma frequency, so that the wave cannot be generated as a whistler mode wave. Consequently, the LF waves generated on the magnetic field of $L=6.7$ in the altitude range from 2000 km to 4700 km are measurable with the PWH onboard the S-520-12 rocket. These analyses support that the observed 139 kHz LF waves by the PWH are generated by the same precipitating electron beams which cause the pulsating aurora near the zenith.

4. Discussion

On the basis of AUREOL/ARCAD 3 satellite observation, BEGHIN *et al.* (1989) reported that downward electron beams of about 100–200 eV energy are responsible for the generation of whistler mode HF emissions down to 1000 km altitude in the nightside auroral region. Therefore it would be appropriate to consider that LF waves accompanied with pulsating aurora are generated by low energy electrons. On the other hand, downward electron beams of several keV to several tens of keV energy are responsible for the emission of pulsating aurora (BRYANT *et al.*, 1971). There are three possible mechanisms for precipitating low energy electrons. In the following we eval-

uate these mechanisms to interpret the result of our correlation analysis.

(1) SAITO *et al.* (1992) suggested that low energy precipitating electrons are the secondary ones caused by acceleration due to the upward propagating kinetic Alfvén wave, which was produced by auroral precipitating electrons and resultant ionization of the neutral atmosphere. In this model, the acceleration region is located at a height of several thousand km. The time necessary for kinetic Alfvén wave to propagate from the ionosphere (100 km) to the acceleration region (lower 10000 km) is approximately 1.2 s, and the time necessary for secondary low energy electrons (100 eV) to precipitate from the acceleration region to the ionosphere is approximately 2.2 s. Therefore the time delay between the primary high energy electrons and the secondary low energy electrons is about 3.4 s. The result of our analysis can not be interpreted by this mechanism.

(2) EVANS *et al.* (1987) suggested that backscattered secondary low energy electrons are produced by primary precipitating high energy electrons and they may bounce between northern and southern hemispheres along geomagnetic field lines. In this model, returned low energy electrons from the opposite hemisphere arrive at the ionosphere more than 20 s later than the first injection of high energy electrons. Therefore this mechanism is unable to explain the present result of our analysis.

(3) DAVIDSON (1990) suggested that the pitch-angle diffusion driven by wave-particle interactions at the equatorial magnetosphere would precipitate morningside electrons with energies greater than several keV. If this process is applicable to both higher energy component causing the auroral emission and lower energy component causing the LF radiation, it is worth estimating their transport time from the equatorial

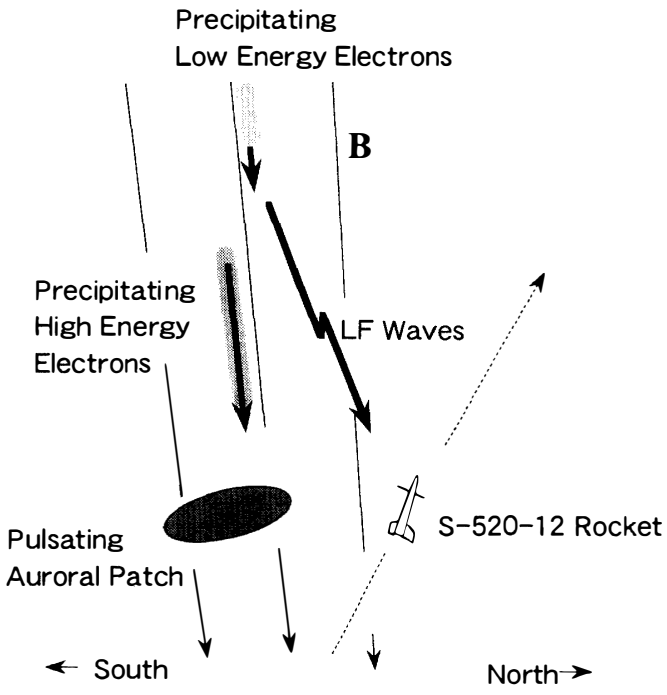

Fig. 10. A schematic illustration of the relationship between precipitating electrons, radiation and propagation of LF waves, location of pulsating patch and rocket position.

magnetosphere to the auroral ionosphere.

Let us suppose that the energy of precipitating high energy electrons is 20 keV, and that the energy of precipitating low energy electrons is 100 eV. Then electrons with 20 keV energy require approximately 0.7 s to travel from the equator of the $L=6.7$ field line to the ionosphere, while electrons with 100 eV energy approximately 9.6 s to travel the same field line. The propagating time for an LF wave from the source region to the ionosphere is at most 0.06 s, therefore this time is negligible. Consequently, low energy electrons lag behind high energy electrons by 9 s. This 9 s time lag approximately agrees with the result of our correlation analysis between LF waves and pulsating aurora. From this evidence, it is strongly suggested that both low energy electrons (100–200 eV) and high energy electrons (several keV to several tens of keV) are simultaneously modulated through the pitch-angle diffusion process in the equatorial magnetosphere. High energy electrons cause the pulsating auroral emission at the ionospheric altitude, whereas low energy electrons generate LF waves at the altitude range of 2000–4700 km and propagate downward. Figure 10 shows a schematic illustration of the relation between precipitating electrons, radiation and propagation of LF waves, location of pulsating patch and rocket position.

5. Conclusion

The observation of pulsating aurora with S-520-12 sounding rocket experiment was successfully carried out at Andøya Rocket Range, Norway on February 26, 1990. On the basis of a correlation analysis between LF wave data measured by the PWH onboard the S-520-12 rocket and auroral image data measured by SIT all-sky TV on the ground, it is possible to interpret a mechanism for pulsating aurora accompanied by pulsating LF wave emission. It is also confirmed that the LF wave radiation has a time lag of about 8 s behind the pulsating auroral emission. We suggest that the LF waves would be caused by precipitating electrons of about 100–200 eV energy modulated near the magnetic equator simultaneously with high energy auroral electrons, and also suggest that high energy electrons would arrive the ionosphere 9 s before low energy electrons because of the velocity dispersion in the precipitating process to the ionosphere. The source altitude of LF waves is suggested to be 2000–4700 km above the pulsating auroral patch, by means of the ray tracing analysis.

Acknowledgments

This study was made using the ARSAD installed at the Aurora Data Center and other equipments at the Information Science Center of the National Institute of Polar Research (NIPR). We sincerely thank Prof. N. SATO, Drs. A. KADOKURA, M. OKADA, H. MINATOYA, K. HASHIMOTO (NIPR), T. ONO and Y. TAKAHASHI (Tohoku Univ.) for their kind suggestions and encouraging discussions. The authors wish to express thanks to all the members of the S-520-12 rocket campaign team.

References

BEGHIN, C., RAUCH, J.L. and BOSQUED, J.M. (1989): Electrostatic plasma waves and HF auroral hiss generated at low altitude. J. Geophys. Res., **94**, 1359–1378.

BENSON, R.F., CALVERT, W. and KLUMPAR, D.M. (1980): Simultaneous wave and particle observations in the auroral kilometric radiation source region. Geophys. Res. Lett., **7**, 959–962.

BRYANT, D.A., COURTIER, G.M. and BENNETT, G. (1971): Equatorial modulation of electrons in a pulsating aurora. J. Atmos. Terr. Phys., **33**, 859–867.

DAVIDSON, G.T. (1990): Pitch-angle diffusion and the origin of temporal and spatial structures in morningside aurorae. Space Sci. Rev., **53**, 45–82.

EVANS, D.S., DAVIDSON, G.T., VOSS, H.D., IMHOF, W.L., MOBILIA, J. and CHIU, Y.T. (1987): Interpretation of electron spectra in morningside pulsating aurorae. J. Geophys. Res., **92**, 12295–12306.

OGUTI, T. (1981): TV observations of auroral arcs. Physics of Auroral Arc Formation, ed. by S.-I. AKASOFU and J.R. KAN. Washington, D.C., Am. Geophys. Union, 31–41 (AGU Monograph, 25).

ROYRVIK, O. and DAVIS, T.N. (1977): Pulsating aurora: Local and global morphology. J. Geophys. Res., **82**, 4720–4740.

SAITO, Y., MACHIDA, S., HIRAHARA, M., MUKAI, T. and MIYAOKA, H. (1992): Rocket observation of electron fluxes over a pulsating aurora. Planet. Space Sci., **40**, 1043–1054.

TSURUDA, K., MACHIDA, S., OGUTI, T., KOKUBUN, S., HAYASHI, K., KITAMURA, T., SAKA, O. and WATANABE, T. (1981): Correlations between the very low frequency chorus and pulsating aurora observed by low-light-level television at $L \simeq 4.4$. Can. J. Phys., **59**, 1042-1048.

TSURUTANI, B.T. and SMITH, E.J. (1974): Postmidnight chorus: a substorm phenomenon. J. Geophys. Res., **79**, 118–127.

WHALEN, B.A., MILLER, J.R. and MCDIARMID, I.B. (1971): Energetic particle measurements in a pulsating aurora. J. Geophys. Res., **76**, 978–986.

YAMAMOTO, T. and OGUTI, T. (1982): Recurrent fast motions of pulsating auroral patches 1. A case study on optical and quantitative characteristics during a slightly active period. J. Geophys. Res., **87**, 7603–7614.

YAU, A.W., WHALEN, B.A. and MCEWEN, D.J. (1981): Rocket-borne measurements of particle pulsation in pulsating aurora. J. Geophys. Res., **86**, 5673–5681.

(Received March 12, 1997; Revised manuscript accepted August 4, 1997)